Available online at www.sciencedirect.com
SCIENCE DIRECT®
Biomass and Bioenergy 27 (2004) 493–505
BIOMASS & BIOENERGY
www.elsevier.com/locate/biombioe

Exhaust gas assisted reforming of rapeseed methyl ester for reduced exhaust emissions of CI engines

A. Tsolakis, A. Megaritis*

School of Engineering, Mechanical and Manufacturing Engineering, The University of Birmingham, Birmingham B15 2TT, UK

Received 6 August 2003; received in revised form 2 April 2004; accepted 21 April 2004

Abstract

The nitrogen oxides (NO_x) emissions of compression ignition (CI) engines fueled with biodiesel are generally higher compared to conventional diesel fuelling. Previous research work in CI engines has shown that the partial replacement of hydrocarbon fuels by hydrogen combined with exhaust gas recirculation (EGR) can reduce NO_x and smoke emissions without significant changes to the engine efficiency. In the present study, the production of hydrogen-rich gas by catalytic exhaust gas assisted fuel reforming of rapeseed methyl ester (RME) has been investigated experimentally as a way to provide the required hydrogen for the reduction of biodiesel emissions. For comparison, tests with ultra low sulphur diesel (ULSD) were also performed. The reforming experiments were carried out in a mini reactor supplied with exhaust gas from a single cylinder CI engine. In all cases, the reactor inlet temperature was kept at 290°C which was chosen as a typical low exhaust gas temperature of diesel engines operating at part load. The engine operating condition (speed, load) was the same in all the tests and the reactor product gas was examined as a function of the reactor fuel flow rate and the composition of fuel and engine exhaust gas. Up to 17% hydrogen content of the reformer product was achieved and the results indicated that the main reactions in the reformer were the exothermic complete oxidation of part of the fuel and the endothermic steam reforming reaction. Reforming of RME produced more hydrogen with higher fuel conversion efficiency compared to ULSD reforming.

Keywords: Biodiesel; Fuel reforming; Exhaust gas; Hydrogen; Engine emissions

1. Introduction

The use of "clean" and renewable fuels may be the key to overcome emission regulations without significant changes to engine efficiency and fuel economy. Pure biodiesel fuel (ester-based oxygenated fuel) and biodiesel/diesel fuel blends have been used in compression ignition (CI) diesel engines without any engine modification. Biodiesel fuel is produced from renewable resources like vegetable oil or animal fat; it is biodegradable and

*Corresponding author. Tel.: +44-121-4144170; fax: +44-121-4143958.
E-mail address: a.megaritis@bham.ac.uk (A. Megaritis).

0961-9534/$ - see front matter © 2004 Elsevier Ltd All rights reserved.
doi:10.1016/j.biombioe.2004.04.007

Nomenclature

ATR	autothermal reforming
B50	blend 50 vol% diesel and biodiesel
BSN	Bosch smoke number
COV	coefficient of variation
EGR	exhaust gas recirculation
G.H.S.V	gas hourly space velocity
H/C	hydrogen to carbon ratio
HHV	higher heating value
IMEP	Indicated mean effective pressure
LHV	lower heating value
LCV	lower calorific value
$\dot{m}$	mass flow rate
NDIR	nondispersive infrared
POX	Partial oxidation
REGR	reformed exhaust gas recirculation
RME	rapeseed methyl ester
SRR	steam reforming reaction
TCD	thermal conductivity detector
ULSD	ultra low sulphur diesel
WGSR	water gas shift reaction
ΔP	reactor pressure drop
n	reforming efficiency (defined Eq. (12))
λ	relative air/fuel ratio

has beneficial effects on engine exhaust emissions when compared to diesel fuel. The oxygen content and the lower calorific value of biodiesel generally result in a measured loss of engine power and an increase of fuel consumption [1,2]. Regarding exhaust emissions, the use of biodiesel results in lower emissions of unburned hydrocarbons, carbon monoxide, smoke and particulate matter with some increase in emissions of NO_x [3,4]. The reasons for the increase of NO_x are still not fully understood. Wang et al. [5] reported that the higher NO_x emissions are mainly due to the shorter ignition delay time when biodiesel is used. The shorter ignition delay, which advances the combustion timing, increases the peak pressure and temperature and enhances NO_x formation, may be attributed to the higher cetane number of biodiesel. Senatore et al. [6], suggested that the higher concentrations of NO_x detected when engines are fueled with biodiesel are primarily due to the operation of the injection system and not the fuel composition (e.g. oxygen content etc.). The use of biodiesel results in advance of the injection timing because of the different densities and bulk modulus of compressibility of diesel and biodiesel and the different quantities of injected fuel mass per cycle. The advance in fuel injection timing with biodiesel has also been confirmed in a recent detailed experimental study by Szybist and Boehman [7].

In previous work carried out at the University of Birmingham [8], the combustion of pure RME or blend with 50% ULSD by volume (referred to as B50) gave an increase of up to 20% and 12% on NO_x emissions, respectively, for the two fuels. The reduction of BSN was up to 60% and 45%, respectively.

The exhaust gas recirculation (EGR) technology is an effective way of reducing NO_x emissions but it is always associated with increased exhaust smoke and particulates as well as fuel consumption [9,10]. On the other hand, as has been shown previously by the authors, the use of EGR combined with hydrogen addition can reduce both NO_x and smoke emissions [8]. With the simultaneous application of EGR and hydrogen enrichment in a CI engine fueled with different mixtures of ULSD and RME, the adverse effects of EGR on smoke could be overcome while still maintaining the reduced NO_x emissions [11].

The substitution of part of the main hydrocarbon fuel by hydrogen has been reported to be beneficial in terms of brake power, thermal efficiency and reduction of HC, CO, CO_2 and particulate emissions. The increased flame speed of hydrogen and thereby increased cylinder peak pressure and temperature tends to increase NO_x emissions except for lean mixtures [12–14]. However, hydrogen can ignite over a wide range of air to fuel ratios and this allows an engine to run leaner, thus leading to less NO_X. Hydrogen combustion can also reduce hot spots that are one of the major contributors to NO_x emissions in internal combustion (IC) engines [15].

The production and/or storage of hydrogen is a problem for both stationary and mobile applications. The storage can be solved by hydrogen-rich gas fuel production (gas which mainly contains H_2, CO, CO_2 and un-reactive hydrocarbons) from liquid or gaseous fuels just before use. A number of investigators have presented various benefits in terms of performance and emissions realised by using reformed fuels rich in hydrogen in engines, e.g. [14,16–18].

There are several techniques already available for *hydrogen* production from reforming of hydrocarbon fuels. In hydrocarbon *steam reforming reaction* (*SRR*), high-temperature steam separates hydrogen from carbon atoms. This process is extremely productive, but it is endothermic and results in a high loss of energy [19]. The reaction for a typical diesel fuel is:

$$C_nH_{1.88n} + nH_2O \rightarrow nCO + 1.94nH_2 \quad (1)$$

where n is the number of carbon atoms in the fuel molecule.

The water–gas shift reaction WGSR can also take place due to the presence of CO and excess steam as a secondary reaction to produce additional hydrogen at reactor temperatures below 750°C [20]:

$$CO + H_2O \rightarrow CO_2 + H_2. \quad (2)$$

Partial oxidation (*POX*) is not usually considered to be attractive in terms of efficiency because it is an exothermic process and the resulting hydrogen containing fuel gas has a lower calorific value than that of the original feed stock [21]. The partial oxidation reaction for diesel fuel is:

$$C_nH_{1.88n} + 0.5nO_2 \rightarrow nCO + 0.94nH_2. \quad (3)$$

Complete oxidation may also take place, which obviously is undesirable in terms of hydrogen production:

$$C_nH_{1.88n} + 1.47nO_2 \rightarrow nCO_2 + 0.94nH_2O. \quad (4)$$

The endothermic 'dry reforming' reaction can also take place at high temperatures (> 800°C) consuming part of the fuel and carbon dioxide to produce more hydrogen:

$$C_nH_{1.88n} + nCO_2 \rightarrow 2nCO + 0.94nH_2. \quad (5)$$

In *autothermal reforming* (*ATR*), the POX and SRR take place in the same reactor. A hydrocarbon fuel feed is reacted with both steam and air or oxygen to produce a hydrogen-rich gas. The reaction for diesel fuel is:

$$C_nH_{1.88n} + xO_2 + (2n - 2x)H_2O \rightarrow nCO_2 + (2n - 2x + 0.94n)H_2 \quad (6)$$

where x is the oxygen to fuel molar ratio.

The SRR reaction absorbs part of the heat generated by the oxidation reaction, limiting the maximum temperature in the reactor. The net result is a slightly exothermic process. An appropriate catalyst is essential to achieve the desired conversion and product selectivity [22].

Thermal decomposition of the hydrocarbon fuel can also result in production of hydrogen at high reactor temperatures:

$$C_nH_{1.88n} \rightarrow nC + 0.94nH_2. \quad (7)$$

Exhaust gas fuel reforming is a combination of all the basic reforming processes, and involves hydrogen generation by direct catalytic interaction of fuel with engine exhaust gases. The application of the technique in IC engines involves the incorporation of a reforming reactor in the conventional EGR system. In this way, the engine is supplied with 'reformed EGR' (REGR), i.e., hydrogen-rich gas. A schematic of the system is shown in Fig. 1.

Earlier work in spark ignition (SI) engines has shown that the use of REGR can provide benefits in terms of combustion quality and emissions [12,23]. The main possible reactions using exhaust gas from SI engines that operate close to stoichiometric conditions ($\lambda = 1$) are the endothermic steam reforming followed by the water gas shift reaction. There is not any considerable amount of oxygen (not more than 1.5%) to carry out any exothermic reaction but there is the maximum percentage of water that can be achieved from the combustion of the fuel (for methane combustion the H_2O percentage in the engine exhaust gas is about 20%). The main problems with the exhaust gas fuel reforming in SI engines are the low engine exhaust gas temperature (temperature below 600°C is not enough for maximum hydrogen yield) and the start-up time of the

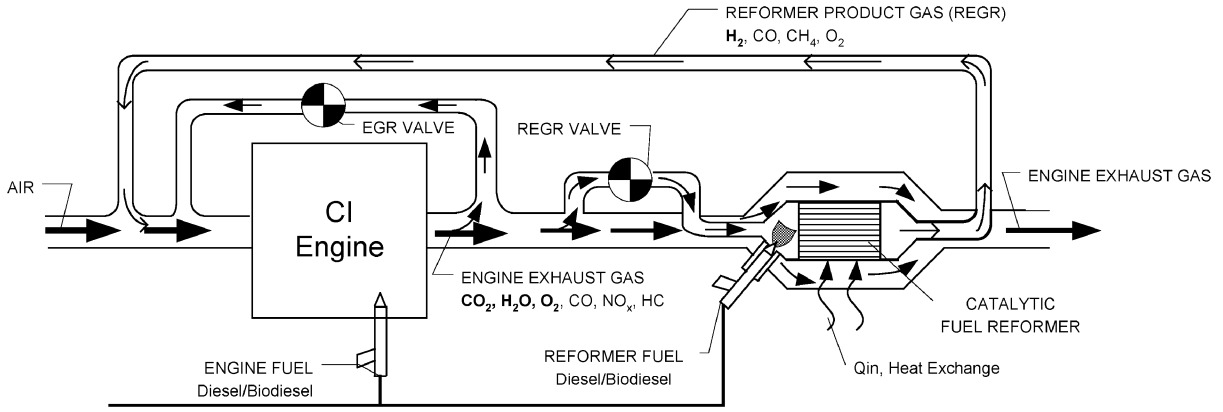

Fig. 1. Schematic of the engine—exhaust gas reformer system.

catalyst. A long start-up time is required since appropriate high exhaust gas temperature needs to be achieved for the endothermic steam reforming to take place.

The exhaust gas fuel reforming in diesel engines is different since the engine operation is always lean and the engine exhaust gas contains a considerable amount of oxygen. The process using diesel engine exhaust gas has many similarities with the autothermal reforming (ATR) described earlier. Both processes have potential to be used in applications that require compact, lightweight hardware capable of processing various fuels. Ahmed and Krumpelt [22] have found that the autothermal reforming of high H/C ratio fuels can produce more hydrogen in the reactor product gas at lower reactor temperatures compared to low H/C ratio fuels. Also the reforming of low H/C ratio fuels is more likely to form coke in the catalyst bed and hence reduce the activity of the catalyst. To avoid coke formation higher steam to fuel ratios (S/F) and reactor temperatures are required.

One of the main advantages of exhaust gas fuel reforming is that there is no need for storage and supply of water and air (oxygen source). The waste heat of the engine exhaust gas is utilised to evaporate the liquid fuel while the water is already in steam form in the exhaust gas and no extra heat is required for water evaporation.

The ATR and the exhaust gas fuel reforming processes can work with different processing rates but in ATR, it is easier to control these rates because of the use of a standard input, i.e., air, steam and fuel. In exhaust gas fuel reforming, the percentages of oxygen and steam in the engine exhaust gas are changing and depend on the engine operating condition (air to fuel ratio) as the diesel engine combustion reaction shows:

$$C_nH_{1.88n} + 1.47n\lambda(O_2 + 79/21N_2) \rightarrow nCO_2 + 0.94nH_2O + 1.47n(\lambda - 1)O_2 + 1.47n\lambda(79/21)N_2. \quad (8)$$

When the engine is fueled with RME, the combustion process and hence the exhaust gas composition are affected due to the different chemical composition and properties (Table 1) of RME compared to diesel fuel. Obviously, the engine operating condition again affects the percentages of steam and oxygen in the exhaust gas as the RME combustion reaction shows:

$$C_nH_{1.85n}O_2 + (1.46n - 1)\lambda(O_2 + 79/21N_2) \rightarrow nCO_2 + 0.92nH_2O + (1.46n - 1)(\lambda - 1)O_2 + (1.46n - 1)\lambda(79/21)N_2. \quad (9)$$

The change of the engine exhaust gas composition affects the rates of the reactants (mainly steam and oxygen) in the reforming reactor as it can be seen from the idealised ULSD and RME exhaust

Table 1
Fuel properties

Fuel analysis	Method	Ultra low sulphur diesel (ULSD)	Rapeseed methyl ester (RME)
Cetane number	ASTM D613	53.9	54.7
Density at 15°C (kg m^{-3})	ASTM D4052	827.1	883.7
Viscosity at 40°C (cSt)	ASTM D445	2.467	4.478
50% distillation (°C)	ASTM D86	264	335
90% distillation (°C)	ASTM D86	329	342
LCV (MJ kg^{-1})		42.7	39
Sulphur (mg kg^{-1})	ASTM D2622	46	5
Aromatics			
Mono (wt%)		21.0	< 0.1
Di (wt%)		3.1	< 0.1
Tri (wt%)		0.3	32.1
Total (wt%)		24.4	32.1
Molecular weight		209	296
C (wt%)		86.5	77.2
H (wt%)		13.5	12.0
O (wt%)		—	10.8

gas fuel reforming reactions:

$$C_nH_{1.88n} + y_1[nCO_2 + 0.94nH_2O + 1.47n(\lambda - 1)O_2 + 1.47n\lambda(79/21)N_2] \rightarrow z_1CO2 + k_1H_2 + 1.47ny_1\lambda(79/21)N_2 \quad (10)$$

$$C_nH_{1.85n}O_2 + y_2[nCO_2 + 0.92nH_2O + (1.46n - 1)(\lambda - 1)O_2 + (1.46n - 1)\lambda(79/21)N_2 \rightarrow z_2CO_2 + k_2H_2 + (1.46n - 1)y_2\lambda(79/21)N_2 \quad (11)$$

where y_1, y_2 are the volumes of exhaust gas required to react stoichiometrically with one unit volume of fuel (gaseous phase), and z_1, z_2 and k_1, k_2 are the number of kmols of carbon dioxide and hydrogen, respectively, in the reactor product gas; subscripts 1 and 2 refer to ULSD and RME, respectively.

As the engine operation shifts closer to stoichiometric ($\lambda = 1$), the percentage of steam in the exhaust increases while the percentage of oxygen decreases. In the extreme case of $\lambda = 1$ the engine exhaust gas contains the maximum percentage of steam of about 12.6% and 12.8% for ULSD and pure RME, respectively, and no oxygen. In this case, the above idealised reforming reactions are similar to steam reforming (Eq. (1)) and a high exhaust temperature is required to drive the endothermic reforming. At idle conditions (very lean combustion) the percentage of oxygen in the engine exhaust is approaching that in the air (about 20%) and the percentage of steam is very small. In this case the idealised reactions (Eqs. (10) and (11)) are very similar to partial or complete oxidation (Eqs. (3) and (4)).

In the present study, the production of hydrogen-rich gas by catalytic exhaust gas fuel reforming of RME was investigated using a laboratory mini reformer at temperatures typical of engine exhaust gas temperatures at part load operation. The efficiency of the exhaust gas reforming process was studied and for comparison, tests with ULSD were also carried out.

2. Experimental

Test engine: The experiments were carried out in a Lister Petter TR1 engine. The engine is an air-cooled, single-cylinder, direct injection, naturally aspirated diesel engine. The main engine specifications are: bore 98.4 mm, stroke 101.6 mm, conrod length 165.0 mm, displacement volume 773 cm^3,

compression ratio 15.5, maximum power 8.6 kW at 2500 rpm and maximum torque 39.2 Nm at 1800 rpm.

Engine instrumentation: An electric dynamometer with a motor and a load cell was used to load and motor the engine. A KISTLER 6125B pressure transducer, mounted flush at the cylinder head and connected via a KISTLER 5011 charge amplifier to a data acquisition board, was used to record the cylinder pressure. The crankshaft position was measured using a digital shaft encoder. The test rig included other standard engine test rig instrumentation such as to allow monitoring of flows (liquid and gaseous fuels, intake air and EGR), temperatures (oil, air, inlet manifold and exhaust) and pressures (gauges mounted at relevant points). Normal engine test bed safety features were also included. Atmospheric conditions (humidity, temperature, pressure) were monitored during the tests.

Data acquisition and analysis were carried out using in-house developed *LabVIEW* based software. Output from the analysis of consecutive engine cycles included peak engine cylinder pressure, indicated mean effective pressure (IMEP), percentage coefficient of variation (% COV) of IMEP, average values and percentage COV of peak pressures, average crank angle for ignition delay, and fuel burn analysis data such as burn duration, 50% burn point etc.

Reforming mini reactor: The reforming tests were conducted in a laboratory mini reformer described previously [23,24]. A schematic of the reactor system is shown in Fig. 2. The reactor was placed in a tubular furnace and the temperature was controlled by means of a temperature controller. A K-type thermocouple was used to record the reactor temperature profile. The thermocouple was placed inside a stainless-steel tube (OD 2.95 mm) fitted in the centre of the reactor. The arrangement allowed vertical movement of the thermocouple and thus monitoring of the reactor temperature profile. A syringe pump fitted with a glass syringe was used to supply the liquid fuel and control the fuel flow rate. The liquid fuel was injected directly into the mini reactor 10 cm above the packed catalyst. The exhaust gas fuel flow into the reactor was measured and controlled

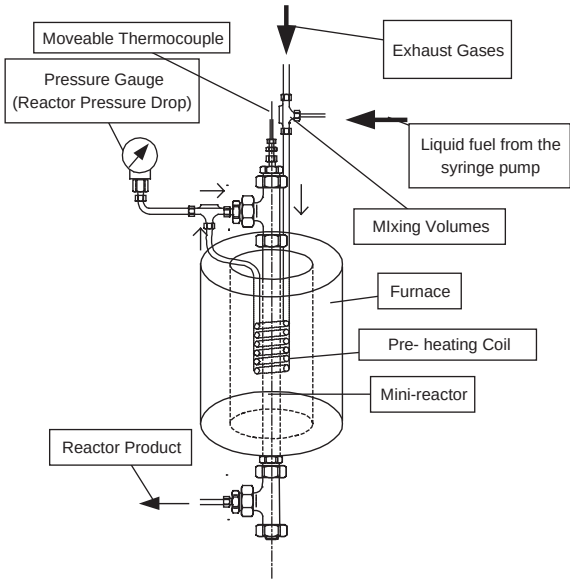

Fig. 2. Schematic of the liquid fuel reforming reactor rig.

by a rotameter. The reactor was loaded with a prototype catalyst provided by Johnson Matthey. The catalyst was a nickel-free formulation, containing precious metal promoted by metal oxides. It was in the form of granules of approximately 1–1.5 mm diameter and it was loaded into the mini reactor tube (ID 10 mm) in three different layers. The catalyst bed weight and length were 4.1 g and 8 cm, respectively. Quartz wool and granular alumina were used to support the catalyst layers and brought the total length to 14 cm.

Exhaust gas emissions and hydrogen analysis: A *HORIBA* analyser model *MEXA*-547GE was used to measure CO, CO_2, unburned hydrocarbons by NDIR method (hexane equivalent), and oxygen concentrations in the exhaust (electrochemical method), together with a *Beckman* 951A chemiluminescence NO/NO_x analyser and a *Beckman* 864 infrared CO_2 analyser. A Hewlett Packard (HP) gas chromatograph equipped with a thermal conductivity detector (TCD) was used for measuring the hydrogen content of the reactor product. A double column arrangement was used; the first column was a 1 m long $\frac{1}{8}$ in diameter Haysep Q, 80–100 mesh and the second a 2 m long $\frac{1}{8}$ in diameter Molesieve 5Å (MS5A). Higher TCD

sensitivity to hydrogen was achieved by using argon as the carrier gas. The H_2 chromatogram area was measured using a HP 3395 integrator.

Fuels: The fuels used were RME and USLD provided by Shell Global Solutions UK. The fuel properties are given in Table 1. RME contains a number of different methyl esters (CH_3OOCR) and the oxygen content of the RME molecule is 10.8 wt%.

Experimental procedure: In all the tests, the engine operating condition was 1500 rpm speed and 6.1 bar IMEP (80% load). First, the mini reactor product gas from the ULSD exhaust gas fuel reforming was examined with the engine operating on ULSD. These tests were carried out to provide a baseline for the RME reforming study. The engine exhaust gas flow rate into the reactor was $8\,l\,min^{-1}$. Four different fuel flow rates were tested; 30, 34, 40 and $55\,ml\,h^{-1}$. Following the tests with ULSD, the mini-reactor product gas composition from the RME exhaust gas fuel reforming was examined. The engine was fueled with pure RME and the exhaust gases ($8\,l\,min^{-1}$) were used for the reforming of RME with flow rates of again 30, 34, 40 and $55\,ml\,h^{-1}$ at the same conditions as in the case of the ULSD tests (temperature and reactor pressure drop).

The mini reactor inlet temperature was set to 290°C (by the furnace temperature controller) for all the reforming tests. The temperature was chosen as a typical low exhaust gas temperature of a diesel engine operating at part load. The gas hourly space velocity (G.H.S.V.; volumetric flow rate of gas per hour divided by the volume of the catalyst bed) was $90,000\,h^{-1}$ approximately, which is typical of automotive three-way catalytic converters. The reactor pressure drop (ΔP) was 0.3 bar (g).

The tests allowed the study of the effects of the different HC fuels (H/C ratio and number of carbons in the molecule) as well as the effects of exhaust gas composition (mainly steam and oxygen) on hydrogen production and fuel conversion efficiency. The reactor product (reformed) gas composition and efficiency were investigated also as a function of the reactant fuel flow rate under the engine operating condition described earlier. The reformed gas composition was monitored over three hours at about every 10 min and the results presented are the average values. No deterioration of the catalyst was observed during the relatively short period of three hours and the measured hydrogen levels were stable throughout the experimentation time in all cases (approximately 1% fluctuation from the average value).

The mini reactor temperature profile first was recorded with only nitrogen flow (unreactive gas); this will be referred to as "reactor temperature". The temperature profile was then recorded under reaction conditions with exhaust gas and fuel flow. The flow in the reactor was the same as that of nitrogen and this temperature profile will be referred to as "reaction temperature". Comparison of the two obtained profiles allowed the study of the sequence of the main reactions (exothermic, endothermic) and the nature of the overall reaction. It has to be noted that the "reaction temperatures" are used as an indication of the temperature profiles and they do not refer to the actual temperatures of the reactant gases, since the thermocouple is placed inside a stainless steel tube (the actual temperatures of the reactant gases could be different from the measured temperature profiles due to heat transfer complications; from the gas to the thermocouple tube and then to the thermocouple).

3. Results and discussion

3.1. Exhaust gas composition from RME and ULSD combustion

Table 2 shows the reactor fuel volumetric and corresponding mass flow rates and the engine exhaust gas composition. The exhaust gas water and oxygen contents (vol%) from the combustion of ULSD and RME are shown for the same engine operating condition described earlier. The engine exhaust gas from the combustion of RME contained higher percentages of water and lower percentages of oxygen compared to ULSD. The engine exhaust gas temperature and the relative air/fuel ratio (λ) are also given in Table 2 for both RME and ULSD fuelling.

Table 2
Exhaust gas fuel reforming conditions

Fuel	Reformer fuel flow rate		Engine exhaust gas 8 l min^{-1} at 85°C				Engine	
	Volume (ml h^{-1})	Mass (g min^{-1})	H_2O (%)	O_2 (%)	Steam (l min^{-1})	O_2 (l min^{-1})	λ	$T_{exhaust}$ (°C)
ULSD	30	0.413	5.95	11.04	0.48	0.88	2.33	350
	34	0.469						
	40	0.551						
	55	0.758						
RME	30	0.448	6.21	10.76	0.50	0.86	2.19	351
	34	0.501						
	40	0.589						
	55	0.810						

3.2. Effects of the engine exhaust gas composition on the reformer product for ULSD reforming

Fig. 3 shows the engine exhaust (E.E.) gas composition when the engine was fueled with ULSD and the reactor product gas composition (dry basis) for the four different ULSD flow rates (with 8 l min^{-1} exhaust gas).

The increase of the fuel flow resulted in an increase of the hydrogen and carbon monoxide contents of the reactor product. Fig. 3 also shows that the percentages of oxygen used and carbon dioxide produced in the reactor were not affected from the increased ULSD flow rate. The CO_2 production and oxygen consumption are believed to be due to complete oxidation of some of the fuel supplied to the reactor.

The CO content of the reactor product gas was always approximately half of the corresponding hydrogen content. Almost all the CO was produced in the reactor since the CO content of the exhaust gas was very low in all cases. The H_2/CO ratio of approximately 2 is very close to that predicted for the steam reforming reaction of diesel (Eq. (1)) and it suggests that the hydrogen was mainly produced by steam reforming.

The increased fuel flow resulted in increased unreacted HCs in the reactor product gas but HCs are combustible and in an engine-reformer closed loop system they will be oxidized in the engine combustion chamber.

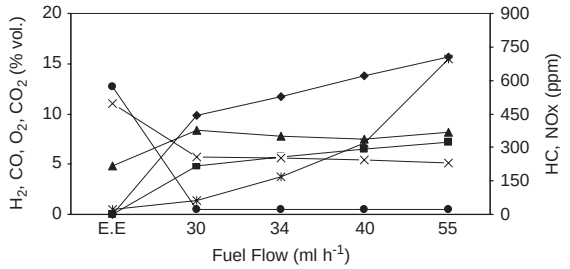

Fig. 3. ULSD exhaust gas reforming. Engine exhaust gas (E.E) and mini-reactor product gas composition. H_2 (♦), CO (■), O_2 (×), NO_X (•), CO_2 (▲), HC (∗).

A secondary reaction that seems to have taken place in the reformer is the reaction of hydrogen with NO_X to give ammonia (NH_3) or nitrogen and water as indicated by the reduction of the NO_X emissions in the reactor for all the tests.

3.3. Effects of the engine exhaust gas composition on the reformer product for RME reforming

Fig. 4 shows the engine exhaust (E.E.) gas composition when the engine was operated with pure RME and the reactor product gas composition (dry basis) for the four different RME fuel flow rates (with 8 l min^{-1} exhaust gas).

The trend of the products is very similar to that shown in Fig. 3 for the ULSD reforming tests. The rise of the fuel flow resulted again in an increased hydrogen and carbon monoxide production. With

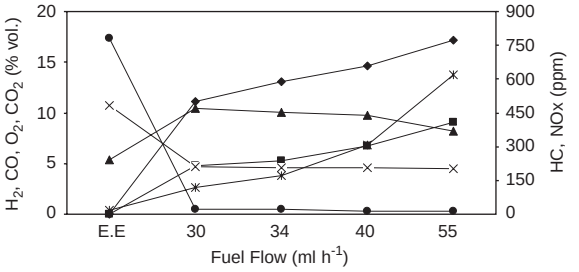

Fig. 4. RME exhaust gas fuel reforming. Engine exhaust gas composition (E.E) and mini-reactor product gas composition. H_2 (♦), CO (■), O_2 (×), NO_X (•), CO_2 (▲), HC (∗).

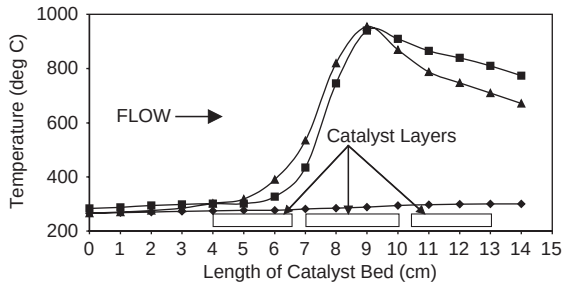

Fig. 5. Reactor temperature profile (N_2 only) (♦) and reaction temperature profiles for 34 ml h^{-1} RME (▲) and ULSD (■) volumetric flow rate.

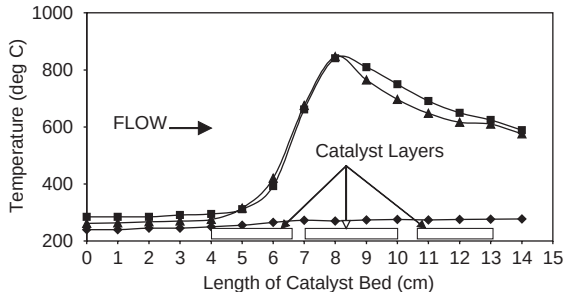

Fig. 6. Reactor temperature profile (N_2 only) (♦) and reaction temperature profiles for 55 ml h^{-1} RME (▲) and ULSD (■) volumetric flow rate.

increased fuel flow, the CO_2 produced in the reactor was reduced slightly while the oxygen consumed was not affected.

Figs. 5 and 6 show the reaction temperature profiles for RME and ULSD reforming for 34 and 55 ml h^{-1} fuel flow, respectively, at a mini-reactor temperature of 290°C. All the reaction temperature profiles show the same sequence of the main reactions in the reformer. A sharp rise of the reaction temperature to between 850 and 950°C due to oxidation occurred first. In this area the fuel was oxidized to produce CO_2 and H_2O and the heat required for the endothermic steam reforming reaction was generated. The new main reactants at high reactor temperature were then the remaining fuel, the steam contained in the engine exhaust gas, and the steam produced in the oxidation area. The CO_2 produced in the oxidation area as well as the exhaust gas CO_2 could have also participated in reactions but such reactions were not evident from the obtained gas compositions at the reactor inlet and outlet. If for example, the dry reforming reaction, given by Eq. (5), had occurred then the H_2/CO ratio would have been different than the obtained ratio of approximately 2 mentioned earlier.

The next area in the catalyst bed is the area where the endothermic steam reforming took place as indicated by the rapid reduction of temperature. The overall reaction as the temperature profiles show was exothermic (as mentioned earlier the measured temperatures were not the actual temperatures of the reactants gases).

The reduction of the temperature in the endothermic area was higher for the RME reforming compared to ULSD (approximately 100 and 60°C difference for the fuel flow rates of 34 and 55 ml h^{-1}, respectively). This is due to the higher amount of steam taking part in the reforming reaction in the case of RME (as explained earlier the percentage of steam in the engine exhaust gas is higher for RME than ULSD). The higher mass flow rate of RME into the reactor compared to ULSD (because of the density difference) as well as heat capacity effects (more CO_2 in the RME exhaust gas) may have also accounted for the larger temperature reduction observed with RME.

Fig. 7 shows the H_2 (%) and CO (%) produced in the mini-reactor from the exhaust gas fuel reforming of RME and ULSD. The reactor product gas from the ULSD reforming contained about 1–2% less hydrogen compared to RME

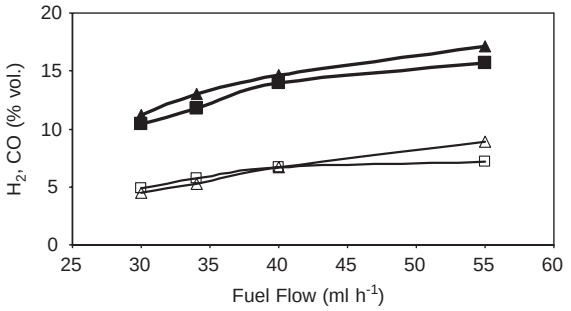

Fig. 7. Hydrogen and carbon monoxide production from the reforming of RME and ULSD. RME reforming: H_2 (▲), CO (△). ULSD reforming: H_2 (■), CO (□).

reforming. Up to 17% hydrogen content of the reformer product was achieved with RME. The CO content of the reactor product for RME reforming was about the same or slightly higher than that for ULSD. The higher yields of hydrogen and carbon monoxide in the reactor product gas from the reforming of RME are due to the higher steam and lower oxygen contents of the RME exhaust gas compared to ULSD (i.e., in the case of RME, more fuel was reformed by steam reforming and less fuel was combusted).

The H/C ratio of the fuel molecule is another parameter that affects the percentage of hydrogen production in the reactor. The H/C ratio of the ULSD molecule is 1.88 while for RME it is slightly lower, 1.85. As reported in the literature, theoretically the higher H/C of the ULSD molecule is beneficial in terms of higher hydrogen yield and better resistant to catalyst deactivation. However, for the tests carried out in this study, the effects of different H/C on hydrogen production could not be compared since the reactant flows were not the same for the two fuels (i.e., different steam and oxygen contents of exhaust gas). Also the small difference in the H/C ratios of the two fuels probably was not enough to give any considerable effects.

3.4. Process efficiency and power losses: effects of fuel and engine exhaust gas composition

Heinzel et al. [25] evaluated the performance of hydrogen generator systems (steam and ATR reformers) in terms of gas process efficiency. They defined the process efficiency as the molar flow rate of hydrogen produced (the entire CO was converted to equivalent H_2) divided by the total fuel flow input (to the reformer and the burner in the case of steam reforming) based on the high heating values (HHV). Ahmed and Krumpelt [22] calculated the theoretical efficiencies for the ATR reforming process of different fuels based on the chemical formula of the fuel only. They defined the efficiency of the fuel processor to convert hydrocarbon fuels (oxygenated and non-oxygenated) into hydrogen as the lower heating value of the hydrogen produced divided by the lower heating value of the fuel used.

Similarly, the process efficiency of the exhaust gas fuel reforming process in this study was determined as the ratio of the chemical power (kW) of the H_2 and CO produced over the chemical power of the fuel fed into the mini-reactor:

$$\eta_{\text{ExhGas Ref}}(\%) = \frac{\text{LCV}_{\text{fuel prod}}\,\dot{m}_{\text{fuel prod}}}{\text{LCV}_{\text{fuel in}}\,\dot{m}_{\text{fuel in}}} \times 100. \tag{12}$$

In a similar way, the power losses in the reformer were calculated as percentages of the reactor fuel input power:

$$\text{Power Losses}\ (\%) = \left(1 - \frac{\text{LCV}_{\text{fuel prod}}\,\dot{m}_{\text{fuel prod}}}{\text{LCV}_{\text{fuel in}}\,\dot{m}_{\text{fuel in}}}\right) \times 100 = 100 - \eta_{\text{ExhGas Ref}}. \tag{13}$$

Fig. 8 shows the power of the gaseous fuel produced in the reactor (Eq. (12) numerator) versus the input chemical power of RME and ULSD fed into the mini reactor (Eq. (12) denominator) for the different fuel volumetric flows tested. For the same fuel volumetric flow rate, the power added to the reactor was higher in the case of the ULSD reforming. This was due to the higher LCV of ULSD (42.7 MJ kg^{-1}) compared to RME (39 MJ kg^{-1}). RME has higher density (883.7 kg m^{-3}) than ULSD (827.1 kg m^{-3}) and hence, the mass flow rate of RME was higher than ULSD for the same volumetric flow rates.

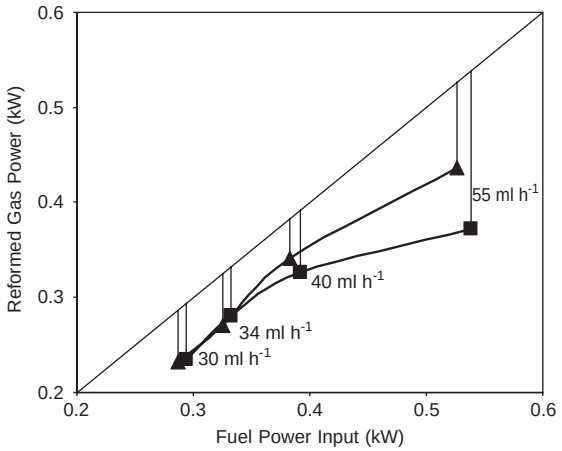

Fig. 8. Chemical power of reformed gas produced by reforming of RME (▲) and ULSD (■). Reactor fuel volumetric flow rates are indicated in ml h^{-1}. The vertical lines joining the points in the graph and the diagonal line indicate the reforming process power losses.

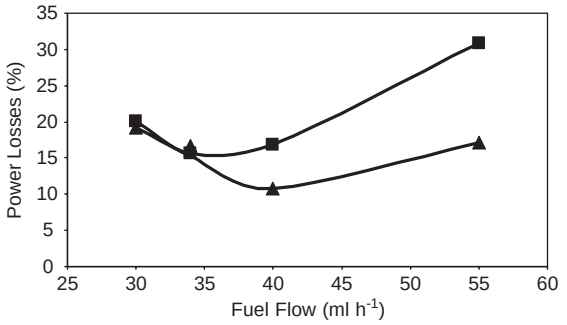

Fig. 9. Power losses (%) in the mini-reactor for the reforming of RME (▲) and ULSD (■).

However, this was not enough to compensate for the lower LCV of RME and the input fuel power for RME was lower than ULSD. The power of the reactor product gas fuel was higher in the case of RME since the percentages of H_2 and CO produced from the reforming of RME were higher than those of ULSD.

The differences between the chemical powers of the reformed gas and the reactor input fuel are the power losses in the reformer. For each reforming test, these power losses are indicated in Fig. 8 by the vertical lines joining the points in the graph and the drawn diagonal line. The latter represents the ideal case of 100% reforming process efficiency. The power losses are also shown in Fig. 9 as percentages of the reactor fuel input power (Eq. (13)). An increase of the fuel flow from 30 to 40 ml h^{-1} resulted in a reduction of power losses (%). However, further increase from 40 to 55 ml h^{-1} resulted in a rise of the losses. With low fuel flow rate, the exothermic reaction (combustion, Eq. (4)) at the first part of the catalyst bed consumed most of the fuel to produce CO_2 and H_2O. As a result, the rest of the fuel was insufficient for the endothermic steam reforming (Eq. (1)) to produce significant amounts of H_2 and CO (excess of steam). As the fuel flow was increased, the amount of fuel used for the exothermic reaction at the first part of the catalyst bed did not change much. This is indicated by the produced carbon dioxide and consumed oxygen in the reactor which were not affected by the fuel flow increase (Figs. 3 and 4). The extra fuel was used for the endothermic steam reforming to produce more H_2 and CO. This is confirmed from the rise of the hydrogen and carbon monoxide contents of the reactor product (Figs. 3 and 4). Since steam reforming is an endothermic reaction, the power (and energy density) of the output fuel gas (H_2 and CO) is higher than the power of the input fuel used for this reaction. This results in a reduction of the overall power losses in the reforming reactor. On the other hand, higher fuel flow rates of more than 40 ml h^{-1} were not beneficial for the reforming process in terms of power losses. Probably, in this case, the quantity of fuel was in excess of that required for all the possible reactions that could take place in the mini-reactor to produce additional hydrogen. Since the un-reacted fuel at the outlet of the mini reactor has not been included in the process efficiency determination (Eq.(12)), the power losses calculated by (Eq. (13)) were increased in the cases of excess fuel into the reactor.

The power losses from the reforming of ULSD were generally higher compared to RME reforming. The reason for this was the higher power of the fuel added to the system and the lower reactor product gas power (i.e., lower reforming efficiency) in the case of ULSD reforming compared to RME (Fig. 8).

Overall, it is clear that with appropriate flow rates of exhaust gas and fuel, the power losses from the conversion of RME and ULSD to hydrogen-rich gas can be reduced considerably. Potentially, power losses of even less than 10% can be achieved with optimisation of the fuel and exhaust gas flow rates into the reforming reactor.

3.5. Discussion: exhaust gas fuel reforming in CI and SI engines

In this section a brief discussion on the application of exhaust gas fuel reforming in IC engines is presented. The discussion is based on the present work on reforming of RME and ULSD for CI engines as well as on previous research on the application of exhaust gas fuel reforming in SI engines fueled with gasoline or methane.

In the SI exhaust gas fuel reforming, the reactor product gas has higher power than the input fed fuel since the main reaction taking place is the endothermic steam reforming and the heat is supplied from the wasted heat of the exhaust gases. However, the steam reforming operating range is limited. The process is beneficial in terms of hydrogen production and efficiency at high engine loads where the exhaust gas temperature is higher than 600°C and the steam reforming can take place. The engine exhaust gas composition in SI engines is not affected much by the engine operating condition (stoichiometric combustion) compared to diesel operation where the exhaust gas water and oxygen contents change considerably at different conditions, as described earlier. Thus, the rates of the reactants (exhaust and fuel) in the SI exhaust gas fuel reforming can be more easily controlled compared to diesel.

On the other hand, the reforming process with diesel engine exhaust gas can take place at much lower temperatures due to the higher oxygen content of the exhaust gas. Combustion of part of the fuel can occur first to increase the reactor temperature so that the other possible reforming reactions can take place. This results in power losses in the fuel conversion process and consequently optimisation of the reactant rates is required in order to reduce or eliminate the power losses. Possibly, an effective way to increase hydrogen production and improve power losses is the addition of water.

The start-up time of the exhaust gas fuel reforming in diesel engine-reformer systems is much shorter compared to the start-up time in spark ignition engines since the fast oxidation reaction takes place first, providing the required heat for the endothermic reactions.

4. Conclusions

1. For production of hydrogen-rich gas, the renewable biodiesel fuel RME as well as diesel fuel can be reformed by exhaust gas assisted fuel reforming at temperatures typical of exhaust gas temperatures of diesel engines operating at part load. Using a prototype catalyst (nickel-free formulation, containing precious metal promoted by metal oxides), up to 17% hydrogen content of the reformer product was achieved at 290°C catalyst bed inlet temperature. The process was found to be mainly a combination of complete oxidation of the fuel at the first part of the catalyst bed followed by endothermic steam reforming.
2. For the same engine–reactor operating condition, the RME reforming produced higher levels of H_2 (by about 1.5%) compared to ULSD reforming. This is due to the higher steam and lower oxygen contents of the RME exhaust gas compared to ULSD.
3. The power losses were lower for the RME fuel conversion to hydrogen-rich gas compared to ULSD conversion.
4. The power losses from the conversion of RME and ULSD to hydrogen-rich gas can be reduced significantly with optimisation of the exhaust gas and fuel flow rates.

Acknowledgements

Support for this work by the Engineering and Physical Science Research Council (Grant Ref. No. GR/R12688), Johnson Matthey Plc, Shell Global Solutions UK and Lister-Petter Ltd. is gratefully acknowledged.

References

[1] Sharp CA, Howell SA, Jobe J. The effect of biodiesel fuel on transient emissions from modern diesel engines, part I regulated emissions and performance. SAE Technical Papers Series 2000, Paper No. 2000-01-1967.

[2] Friis HK, Grouleff JM. Chemical and biological characteristics of exhaust emissions from a DI diesel engine fueled with rapeseed oil methyl ester (RME). SAE Technical Papers Series 1997, Paper No. 971689.

[3] Graboski MS, Ross JD, McCormick RL. Transient emissions from No. 2 diesel and biodiesel blends in a DDC Series 60 engine. SAE Technical Papers Series 1996, Paper No. 961166.

[4] Marshall W, Schumacher GL, Howell S. Engine exhaust emissions evaluation of a Cummins L10E when fueled with a biodiesel blend. SAE Technical Papers Series 1995, Paper No. 952363.

[5] Wang WG, Lyons DW, Clark NN, Gautam M, Norton PM. Emissions from nine heavy trucks fueled by diesel and biodiesel blend without engine modification. Environmental Science and Technology 2000;34(6):933–9.

[6] Senatore A, Cardone M, Rocco V, Prati MV. A comparative analysis of combustion process in a D.I. diesel engine fueled with biodiesel and diesel fuel. SAE Technical Papers Series 2000, Paper No. 2000-01-0691.

[7] Szybist JP, Boehman AL. Behavior of a diesel injection system with biodiesel fuel. SAE Technical Papers Series 2003, Paper No. 2003-01-1039.

[8] Tsolakis A, Megaritis A, Wyszynski ML. Effects of reformed EGR on the diesel engine smoke-NO_x emissions trade-off. Proceedings of the nineth Postgraduate Research Symposium, School of Engineering, The University of Birmingham, 2003. p. 30–4. ISBN 0704424150.

[9] Ladommatos N, Balian R, Horrocks R, Cooper L. The effect of exhaust gas recirculation on soot formation in a high-speed direct-injection diesel engine. SAE Technical Papers Series 1996, Paper No. 960841.

[10] Ladommatos N, Balian R, Horrocks R, Cooper L. The effect of exhaust gas recirculation on combustion and NO_x emissions in a high-speed direct-injection diesel engine. SAE Technical Papers Series 1996, Paper No. 960840.

[11] Teo LKS, Tsolakis A, Megaritis A, Wyszynski ML. Hydrogen and biodiesel mixtures as fuels for the compression ignition engine. Proceedings of the second International Conference on Thermodynamic Processes in Diesel Engines (THIESEL), Valencia, Spain. 2002. p. 389–95. ISBN 84-9705-233-1.

[12] Jamal Y, Wyszynski ML. On-board generation of hydrogen rich fuels—a review. International Journal of Hydrogen Energy 1994;19(7):557–72.

[13] Apostolescu N, Chiriac R. A study of combustion of hydrogen-enriched gasoline in a spark ignition engine. SAE Technical Papers Series 1996, Paper No. 960603.

[14] Andreatta D, Dibble RW. An experimental study of air-reformed natural gas in spark-ignited engines. SAE Technical Papers Series 1996, Paper No. 960852.

[15] Heywood JB. Internal combustion engine fundamentals. New York: McGraw-Hill; 1988(ISBN 0-07-100499-8).

[16] Shrestha SOB, LeBlanc G, Balan G, De Souza M. Before treatment method for reduction of emissions in diesel engines. SAE Technical Papers Series 2000, Paper No. 2000-01-2791.

[17] Sogaard C, Schramm J, Jensen TK. Reduction of UHC-emissions from a natural gas fired SI engine—production and application of steam reforming natural gas. SAE Technical Papers Series 2000, Paper No. 2000-01-2823.

[18] Kirwan JE, Quader AA, Grieve MJ. Advanced engine management using on-board gasoline partial oxidation reforming for meeting super-ULEV (SULEV) emissions standards. SAE Technical Papers Series 1999, Paper No. 1999-01-2927.

[19] Steban RF, Parks FB. Emission control with lean operation using hydrogen supplemented fuel. SAE Technical Papers Series 1974, Paper No. 740184.

[20] Traxel BE, Hohn KL. Partial oxidation of methanol at milliseconds contact times. Applied Catalysis A: General 2003;244(1):129–40.

[21] Houseman J, Hoehn FW. A two-charge engine concept: hydrogen enrichment. SAE Technical Papers Series 1974, No. 741169.

[22] Ahmed S, Krumpelt M. Hydrogen from hydrocarbon fuels for fuel cells. International Journal of Hydrogen Energy 2001;26(4):291–301.

[23] Allenby S, Chang WC, Megaritis A, Wyszynski ML. Hydrogen enrichment: a way to maintain combustion stability in a natural gas fueled engine with exhaust gas recirculation the potential of fuel reforming. Proceedings of the Institution of Mechanical Engineers Part D 2001;215:405–18.

[24] Tsolakis A, Megaritis A, Wyszynski ML. Application of exhaust gas fuel reforming in compression ignition engines fueled by diesel and biodiesel fuel mixtures. Energy & Fuels 2003;17(6):1464–73.

[25] Heinzel A, Vogel B, Hubner P. Reforming of natural gas—hydrogen generation for small scale stationary fuel cell systems. Journal of Power Sources 2002;105(2):202–7.